



## Multielement adsorption of metal ions using Tururi fibers (*Manicaria Saccifera*): experiments, mathematical modeling and numerical simulation

Carla B. Vidal<sup>a,\*</sup>, Diego Q. Melo<sup>b,c</sup>, Giselle S.C. Raulino<sup>a</sup>, Adriana D. da Luz<sup>d</sup>, Cleuzir da Luz<sup>e</sup>, Ronaldo F. Nascimento<sup>a,b</sup>

<sup>a</sup>Department of Hydraulic and Environmental Engineering, Federal University of Ceará, Rua do Contorno, S/N Campus do Pici, Bl. 713 CEP. 60451-970 Fortaleza, Ceará, Brazil, Tel. +55 85 3366 9042; emails: [carlab.vidal@gmail.com](mailto:carlab.vidal@gmail.com) (C.B. Vidal), [gisellescr@yahoo.com.br](mailto:gisellescr@yahoo.com.br) (G.S.C. Raulino), [ronaldo@ufc.br](mailto:ronaldo@ufc.br) (R.F. Nascimento)

<sup>b</sup>Department of Analytical Chemistry and Physical Chemistry, Federal University of Ceará, Rua do Contorno, S/N, Campus do Pici, Bl. 940 CEP, 60451-970 Fortaleza, Ceará, Brazil, email: [diegodqm@gmail.com](mailto:diegodqm@gmail.com) (D.Q. Melo)

<sup>c</sup>Department of Chemistry, Instituto Federal de Educação e Ciência do Piauí, Paulistana, Piauí, Brazil

<sup>d</sup>Department of Environmental Engineering, Federal University of Fronteira Sul, Rua Major Antônio Cardoso, 590, Centro CEP: 89870000, Cerro Largo, Rio Grande do Sul, Brazil, email: [adriana.luz@uffs.edu.br](mailto:adriana.luz@uffs.edu.br)

<sup>e</sup>Department of Food Engineering, State University of Santa Catarina, Pinhalzinho, Santa Catarina, Brazil, email: [cleuzir@udesc.br](mailto:cleuzir@udesc.br)

Received 28 December 2014; Accepted 27 February 2015

### ABSTRACT

A numerical and experimental study of the multielement adsorption of Cd<sup>2+</sup>, Cu<sup>2+</sup>, Ni<sup>2+</sup>, and Pb<sup>2+</sup> metal ions in batch and column system were carried out in aqueous solution using Tururi fibers as adsorbent. The kinetics and thermodynamic equilibrium parameters were studied. The adsorption kinetics was fitted to the homogeneous diffusion model and the results showed good linear correlation coefficients. Furthermore, a mathematical model was built to describe the mass transfer kinetics for fixed bed column tests. The effects of constant adsorption equilibrium, external mass transfer, and intraparticle diffusion resistance on breakthrough curves were studied. The equations which describe the phenomenology were discretized using the finite volumes method with the weight upstream differencing scheme and central difference scheme formulations. The results for the breakthrough curves obtained through simulation showed good agreement compared with the experimental data.

*Keywords:* Adsorption; Metal ions; Tururi fibers; Mathematical modeling

### 1. Introduction

Toxic metals are continuously used in industrial activities, contaminating aquatic environments and may be present in toxic concentrations in the air due to the incineration of municipal and industrial wastes [1]. The non-degradability, toxicity, carcinogenic, or

mutagenic effects of these pollutants has received special attention, even when these pollutants are present in very low concentrations. The removal and recovery of toxic metals are very important with regard to economic matters and especially environmental. Consequently, the implementation of removal technologies for the treatment of effluents from various industries (mining, textile, painting, electroplating,

\*Corresponding author.

pesticide-producing, petrochemical) has become a matter of urgency, since in many cases, the effluents are discarded into water bodies with no suitable treatment [2,3].

However, the majorities of methods have limitations such as high operating costs, incomplete removal of metal ions; in addition to generating secondary pollution such as sludge by precipitation with sodium hydroxide. Adsorption using lignocellulose-derived material has been studied as adsorbents including cellulosic substrates [4], sugar cane bagasse [5], cashew bagasse [6], and coconut shell [7]. A major advantage of using natural fibers as adsorbents is the ready availability of renewable sources in nature, the low costs, the biodegradability, as well as the excellent mechanical properties.

Natural fibers of vegetable origin, mostly agricultural wastes are an abundant biomass consisting of cellulose, hemicellulose, pectin, lignin, and protein. These compounds have a large number of functional groups that can adsorb certain contaminants present in water [4–7]. Originally from the Amazon estuary, the palm of ubuçu (*Manicaria Saccifera*) carries fruits protected by a fibrous sheath called “Tururi”. Despite the fact that this fiber has economic importance in a number of commercial sectors, there are no studies known on its physical and chemical properties for potential use in adsorption processes. A major advantage of using natural fibers as adsorbents is the ready availability of renewable sources in nature, the low costs, the biodegradability as well as the excellent mechanical properties.

In this context, the aim of this research is to study the equilibrium and kinetics of the metal ions in water phase, using Tururi fibers as adsorbent, and thus use the parameters obtained from experimental tests for simulation of the metal ions breakthrough curves in fixed bed column. The mathematical model used is a cluster model of pore diffusion which considers the internal and external resistances to mass transfer to the adsorbent particles. The finite volume method was used in the discretization of the equations with the interpolation function weight upstream differencing scheme (WUDS) along the column and the central difference scheme (CDS) along the particle and the algorithm was implemented in the FORTRAN programming language.

## 2. Materials and methods

Analytical-grade chemicals and ultrapure water (Millipore Direct Q3 Water Purification System) were used to prepare the solutions. Multielement stock

solutions of  $\text{Cd}^{2+}$ ,  $\text{Cu}^{2+}$ ,  $\text{Ni}^{2+}$ , and  $\text{Pb}^{2+}$  ( $500 \text{ mg L}^{-1}$ ) were prepared with  $\text{Cd}(\text{NO}_3)_2 \cdot 4\text{H}_2\text{O}$ ,  $\text{Cu}(\text{NO}_3)_2 \cdot 3\text{H}_2\text{O}$ ,  $\text{Ni}(\text{NO}_3)_2 \cdot 6\text{H}_2\text{O}$ , and  $\text{Pb}(\text{NO}_3)_2$  (Merck, São Paulo, Brazil), respectively. The acetate buffer was prepared with sodium acetate and glacial acetic acid.  $\text{NaOH}$  ( $0.10 \text{ mol L}^{-1}$ ) and  $\text{HCl}$  ( $0.10 \text{ mol L}^{-1}$ ) solutions were used for pH adjustments. Tururi fibers were supplied by Embrapa Tropical Agro-industry, CE, Brazil (EMBRAPA/CE).

During the adsorption isotherms,  $50.0 \text{ mg}$  of the adsorbent was added to Erlenmeyer flasks ( $50.0 \text{ mL}$ ) containing the metal ions solutions ( $25.0 \text{ mL}$ ) that was shaken using an orbital shaker device (Marconi, Brazil) operating at  $200 \text{ rpm}$  ( $28 \pm 2^\circ\text{C}$ ). The experiments were performed in duplicate and the concentration range varying from  $20$  to  $500 \text{ mg L}^{-1}$ . The solution pH was adjusted to  $5.5$ . The equilibrium adsorption capacities were calculated using Eq. (1):

$$q_e = \frac{V(C_o - C_e)}{M} \quad (1)$$

where  $q_e$  is the equilibrium adsorption capacity ( $\text{mg of metal/g adsorbent}$ ),  $C_o$  is the initial concentration of the metal ion ( $\text{mg L}^{-1}$ ),  $C_e$  is the equilibrium concentration of metal ion ( $\text{mg L}^{-1}$ ),  $V$  is the volume of the solution ( $\text{L}$ ), and  $M$  is the mass of adsorbent ( $\text{g}$ ). Control experiments were carried out in the absence of adsorbent to check for any adsorption on the walls of the flasks. The Langmuir multielement isotherm model was used to fit the experimental data [8].

Adsorption kinetics allows to evaluate the extent of removal of metal ions as well as to identify the prevailing mechanisms involved in the adsorption process. A multielement solution of  $\text{Cd}^{2+}$ ,  $\text{Cu}^{2+}$ ,  $\text{Ni}^{2+}$ , and  $\text{Pb}^{2+}$  ( $100.0 \text{ mg L}^{-1}$  each) was continuously shaken ( $200 \text{ rpm}$ ) at  $\text{pH } 5.5$  and the temperature was kept at  $28 \pm 2^\circ\text{C}$ . Aliquots of the supernatant were collected at regular time intervals, up to  $60 \text{ min}$ . The experimental data of the adsorption kinetics of the multielement metal ions were adjusted by the homogenous diffusion model in particle according to Eq. (2) [9].

$$\frac{\partial q}{\partial t} = \frac{1}{r^2} \frac{\partial}{\partial r} \left\{ r^2 D_{\text{ef}} \frac{\partial q}{\partial r} \right\} \quad (2)$$

with the following boundary conditions (BC):

$$q(r, 0) = q_0; \quad q(r, t) = q_0; \quad \left. \frac{\partial q}{\partial r} \right|_{r=0} = 0 \quad (2a)$$

where  $r$  is the position in the radius from the center of the particle considered to be spherical,  $t$  is the time, and  $D_{\text{ef}}$  is the effective diffusivity coefficient.

An adsorption column (9.5 cm height and 1.0 cm diameter) was prepared using 2 g of the adsorbent. About 160 mL of the multielement solution (300 mg L<sup>-1</sup>) was passed through the column at a flow rate of 2.0 mL min<sup>-1</sup> and 4 mL samples were collected at the outlet of the column prior to analyses [10].

The mathematical model is a grouped model of diffusion in the pores, which considers the mass transfer resistance inside and outside the particle adsorbent. Mathematical modeling of this process involves the equations of chemical species conservation in the liquid and solid phases, which describe the solute concentration inside the column and the particle with respect to time and position, as well as initial BC. The surface diffusion coefficient ( $D_s$ ) was assumed to increase exponentially with surface coverage according to Eq. (3).

$$D_s(q) = D_{ef} \exp \left[ k \left( \frac{q}{q_{sat}} \right) \right] \quad (3)$$

where  $D_{ef}$  is the diffusion coefficient at  $q = 0$ ,  $k$  is a parameter of Eq. (3) related to diffusion,  $q$  is the concentration of the solute in the solid phase, and  $q_{sat}$  is the saturation concentration of the solute at the surface. Eq. (3) was incorporated into the adsorption model to take into account the variation in the surface diffusion coefficient  $D_s$  as a function of time and position within the particles [11]. Setting  $k = 0$  in Eq. (3) also allowed for the use of a constant (concentration independent)  $D_s$ .

In this case, the concentration of the solute in the liquid phase,  $C$ , varies with the axial position  $z$  and the time  $t$ , while the concentration in the solid phase  $q$  is a function of the radial position  $r$  inside the particle. Assuming an isothermal process because of the high heat capacity of water; spherical adsorbent particles, and fast adsorption kinetics, the solute mass balance in the solid phase is given by Eq. (4).

$$\frac{\partial q}{\partial t} = \frac{D_{ef}}{r^2} \frac{\partial}{\partial r} \left\{ r^2 \exp \left[ k \frac{q}{q_{sat}} \right] \frac{\partial q}{\partial r} \right\} \quad (4)$$

With the following initial (IC) and BC:

$$\text{IC} : t = 0, 0 \leq r \leq R, 0 \leq z \leq L, q_i = 0 \quad (4a)$$

$$\text{BC1} : t > 0, 0 \leq z \leq L, \left. \frac{\partial q}{\partial r} \right|_{r=0} = 0 \quad (4b)$$

$$\text{BC2} : t > 0, 0 \leq z \leq L, D_{ef} \rho_s \exp \left[ k \left( \frac{q}{q_{sat}} \right) \right] \left. \frac{\partial q}{\partial r} \right|_{r=R} = k_f (C - C_e) \quad (4c)$$

where  $\rho_s$  is the solid density,  $k_f$  is the external mass transfer coefficient, and  $C_e$  is the solute concentration in the liquid phase at the solid–liquid interface. The initial condition used to describe the model for solid phase requires, along the bed at time zero, the concentration in the solid phase equal to zero for adsorption. The BC employed in the model are symmetry and equality of flows.

In the absence of axial solute dispersion in the bed, the solute mass balance in the fluid phase along with the relevant IC and BC is expressed by Eq. (5), where in (5a) and (5b) are the initial condition and the boundary condition, respectively, for this equation.

$$\frac{\partial C}{\partial t} = - \frac{v_s}{\varepsilon} \frac{\partial C}{\partial z} - \frac{3(1-\varepsilon)}{R} \frac{k_f}{\varepsilon} (C - C_e) \quad (5)$$

$$\text{IC} : t = 0, 0 \leq z \leq L, C = 0 \quad (5a)$$

$$\text{BC} : t > 0, z = 0, C = C_{in}(t) \quad (5b)$$

where  $v_s$  is the superficial velocity of the liquid in the bed,  $\varepsilon$  is the bed porosity, and  $R$  is the radius of the adsorbent particle. The time-varying BC at the bed inlet in Eq. (5b) was employed primarily to lend greater flexibility to the model, so that it can handle experiments under variable influent-concentration conditions. However, this feature of the model also allowed for the successful description of discontinuities in the experimental breakthrough curves caused by small variations of the influent concentration  $C_{in}$ , with time due to the batch wise production of feed solution. Because of the assumption of fast intrinsic adsorption kinetics, the solid-phase and liquid-phase solute concentrations at the solid–liquid interface can be related through the equilibrium isotherm.

The finite volume method was used to discretize the conservation equations. The choice is due to the fact that it ensures the conservation of the quantities involved, both at the elementary level and globally. In this work, we used the explicit formulation and one-dimensional (1D) structured mesh for storing discrete points [8]. In the computational mesh, we used a co-located arrangement of variables, where all variables are stored in the center of the control volumes. For the evaluation of the variables and their derivatives on the faces of the control volumes, the WUDS

along the column and the CDS throughout the particle were applied.

The X-ray fluorescence analyses (XRF) were determined in order to procedure the characterization of the Tururi fiber before and after adsorption of metal ions. The method was characterized using a wavelength dispersive X-ray fluorescence spectrometer (model ZMS Mini II, Rigaku).

### 3. Results and discussion

The adsorption kinetics is expressed as the solute removal rates that control the residence time of the adsorbate in the solid–solution interface [12]. The equilibrium times found for the adsorption of metal ions on Tururi fibers were instantaneous for all the metal ions (Fig. 1).

Kinetic modeling of metal adsorption is important since the effectiveness of the adsorption process for metal ions removal from aqueous solutions strongly depends on the sorption dynamics. Predicting the rate at which sorption takes place in a given system is one of the crucial factors in adsorption system design [13]. In this work, the diffusion coefficients were obtained from Eq. (2) and the results were  $D_{\text{efNi}} = 0.0016$ ;  $D_{\text{efCu}} = 0.0089$ ;  $D_{\text{efCd}} = 0.0016$ ;  $D_{\text{efPb}} = 0.0077 \text{ cm}^2 \text{ s}^{-1}$ . According to the  $D_{\text{ef}}$  values obtained from the model, it is possible to notice that  $\text{Cu}^{2+}$  and  $\text{Pb}^{2+}$  values are higher than the other two metal ions; this could be related to its higher adsorption capacities compared to the other two metal ions adsorption capacities.

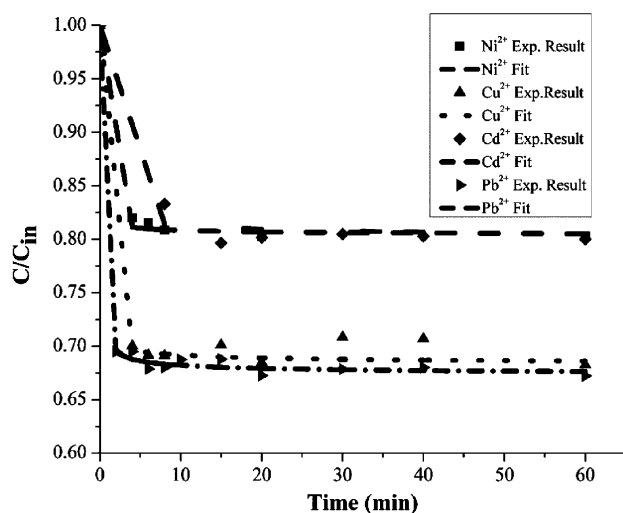


Fig. 1. Multielement adsorption kinetics of metal ions and adjustment of effective diffusivity ( $D_{\text{ef}}$ ). Conditions:  $100 \text{ mg L}^{-1}$ ;  $M = 50.0 \text{ mg}$ ;  $V = 25 \text{ mL}$  at  $28 \pm 2^\circ \text{C}$ .

The presence of polar functional groups including carboxylic, hydroxyl, and phenolic acid groups [14,15] in Tururi fibers can be involved in metal binding by ion exchange between protons present in the biomass and metal ions taken up from water or complexation mechanism interaction. Sousa Neto and coworkers [15] studied the removal of the same metal ions studied in the present work using green coconut shell as adsorbent and the authors also found a fast kinetic process with 90% of metal ions adsorbed within 80 min. According to them, the mechanisms responsible to the metal uptake by vegetal biomaterials involve ion exchange, surface adsorption, chemisorption, complexation, and adsorption–complexation processes.

The equations that describe the adsorption of metals ions ( $\text{Cu}^{2+}$ ,  $\text{Cd}^{2+}$ ,  $\text{Ni}^{2+}$ , and  $\text{Pb}^{2+}$ ) in the multielement solution using a fixed bed column were solved aiming to validate the proposed mathematical model and numerical methodology developed. The results obtained by simulation are compared with the experimental data. The input parameters of the model to determine the concentration profiles of ions metal in the mixture and the parameters used to obtain the multicomponent breakthrough curves of metal ions on Tururi fibers are shown in Table 1.

Fig. 2 shows the breakthrough curve of metal ions, using the mathematical model. The numerical results in Fig. 2 presented a deviation in relation to the experimental data for the multielement breakthrough curves.

This deviation can be related to the Biot number, which is an adimensional number and it represents the relation between the resistance to internal and external mass transfer [16]. In the present work, the following Biot numbers were found for the metal ions:  $\text{Bi}_{\text{Cd}} = 10.23$ ;  $\text{Bi}_{\text{Ni}} = 9.90$ ;  $\text{Bi}_{\text{Cu}} = 9.50$  and  $\text{Bi}_{\text{Pb}} = 2.56$ .

According to Sulaymon and Ahamed [16], as the average Biot number increases for each solute, the competitive adsorption rate will decrease and the form of the breakthrough curves will be flatter and there will be a lower break point. This is due to the low intraparticle resistance and also the reduction in the contact time required to reach saturation. With an increase in the bed height, the competitive adsorption rate will increase and the shift of the weak components will be greater, leading to a breakthrough curve with a higher breakpoint.

The competitive adsorption rate will decrease as the average Biot number increases for each adsorbate, leading to a lower breakpoint because of the low intraparticle resistance and the reduction in the contact time. The increase in the bed height leads to an increase in the competitive adsorption rate, and the displacement of the weak components will be greater.

Table 1

Parameters used to obtain the multicomponent breakthrough curves of metal ions on Tururi

Parameters	Cu <sup>2+</sup>	Cd <sup>2+</sup>	Ni <sup>2+</sup>	Pb <sup>2+</sup>
C <sub>in</sub> (mg L <sup>-1</sup> )	276.72	299.53	306.53	303.70
ε <sub>L</sub>	0.73	0.73	0.73	0.73
D <sub>m</sub> (cm <sup>2</sup> s <sup>-1</sup> )	7.13 × 10 <sup>-6</sup>	7.17 × 10 <sup>-6</sup>	6.79 × 10 <sup>-6</sup>	9.25 × 10 <sup>-6</sup>
D <sub>eff</sub> (cm <sup>2</sup> s <sup>-1</sup> )	8.9 × 10 <sup>-3</sup>	1.634 × 10 <sup>-3</sup>	1.632 × 10 <sup>-3</sup>	7.743 × 10 <sup>-3</sup>
ρ <sub>s</sub> (g L <sup>-1</sup> )	635.75	635.75	635.75	635.75
d <sub>p</sub> (cm)	0.059	0.059	0.059	0.059
d <sub>c</sub> (cm)	1.0	1.0	1.0	1.0
Q (mL min <sup>-1</sup> )	4.0	4.0	4.0	4.0
L (cm)	9.5	9.5	9.5	9.5
b(L g <sup>-1</sup> )	0.005	0.006	0.015	0.002
q <sub>max</sub> (mg g <sup>-1</sup> )	104.03	126.75	48.83	52.59
k <sub>f</sub>	1.76 × 10 <sup>-3</sup>	1.76 × 10 <sup>-3</sup>	1.70 × 10 <sup>-3</sup>	2.09 × 10 <sup>-3</sup>

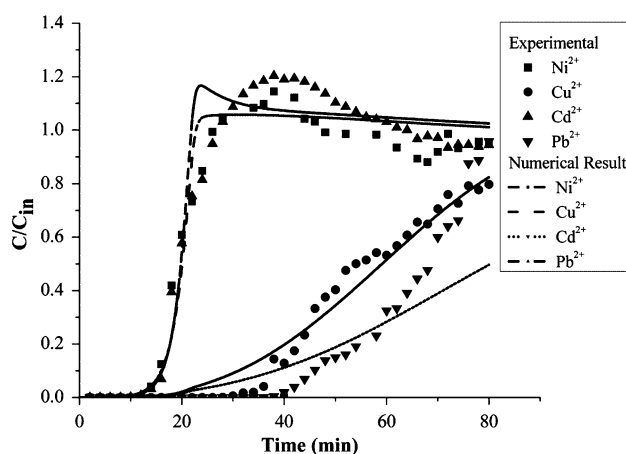


Fig. 2. Experimental and simulated breakthrough curves of metal ions.

A lower Biot number was observed for Pb<sup>2+</sup>, where a higher intraparticle diffusivity of this metal ion occurs compared with the others. This corroborates the mathematical model and the numerical methodology used, demonstrating that they represent the real adsorption process with good accuracy and allowing other situations to be simulated. According to Cooney [17], the external mass transfer is totally dominating at Bi < 0.5, while the adsorption process is limited by intraparticle diffusion for Bi > 30.

In order to predict the operating conditions of the adsorption process, it was performed a sensitivity parametric analysis of the operational conditions. The parameters studied include volumetric flow, bed height, and bed porosity. A numerical experiment was performed for three cases specified in Table 2 for the parameters shown in Table 1. The parameters' values

Table 2

Operational conditions used in the numerical simulations with initial conditions: C<sub>in</sub> = 300 mg L<sup>-1</sup> compared to real conditions: flow = 4 mL min<sup>-1</sup>; bed height = 9.5 cm and ε = 0.73)

Case	Adsorbate	Flow (mL min <sup>-1</sup> )	Bed height (cm)	Porosity (ε)
1	Cu <sup>2+</sup>	8	9.5	0.73
	Cd <sup>2+</sup>	8	9.5	0.73
	Ni <sup>2+</sup>	8	9.5	0.73
	Pb <sup>2+</sup>	8	9.5	0.73
2	Cu <sup>2+</sup>	4	6.5	0.73
	Cd <sup>2+</sup>	4	6.5	0.73
	Ni <sup>2+</sup>	4	6.5	0.73
	Pb <sup>2+</sup>	4	6.5	0.73
3	Cu <sup>2+</sup>	4	9.5	0.53
	Cd <sup>2+</sup>	4	9.5	0.53
	Ni <sup>2+</sup>	4	9.5	0.53
	Pb <sup>2+</sup>	4	9.5	0.53

chose to evaluate the performance of the column process were due in accordance with others from the literature [8,18].

Fig. 3 shows the numerical results of the multielement breakthrough curves using initial concentrations, of C<sub>in</sub> 300 mg L<sup>-1</sup> for each contaminant in the mixture, a volumetric flow of 4 mL min<sup>-1</sup>, and porosity of 0.73 for two different bed heights (L = 9.5 and 6.5 cm). The breakthrough times of the metal ions increased with the increasing in the bed height. According to Vidal et al. [8], the higher the bed height of the adsorbent is the longer the service time of the column will be, taking into account that the surface area of the material increases as the number of active sites available for interaction of adsorbate–adsorbent increases.

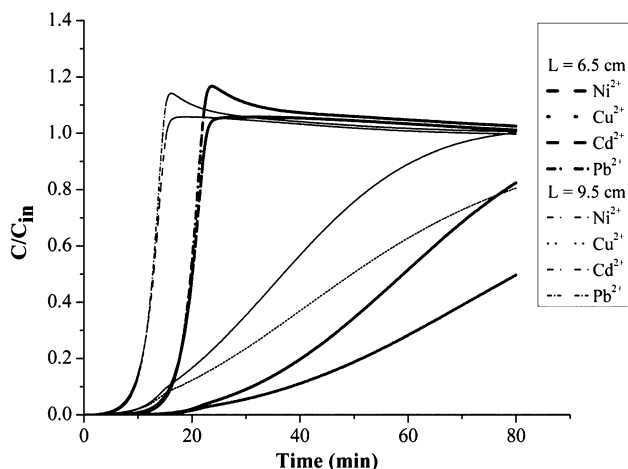


Fig. 3. Numerical results of the multielement breakthrough curves of the metal ions studied for different bed heights ( $L$ ). Initial conditions:  $C_{in} = 300 \text{ mg L}^{-1}$ ;  $Q = 4 \text{ mL min}^{-1}$  and  $\varepsilon = 0.73$ .

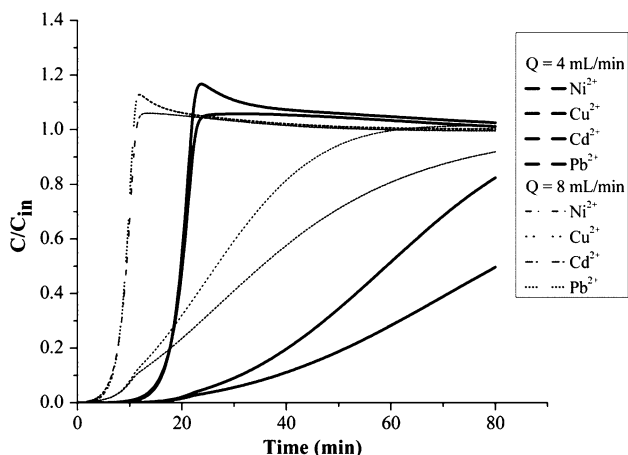


Fig. 4. Multielement breakthrough curves of the metal ions for two different flows. Initial conditions:  $C_{in} = 300 \text{ mg L}^{-1}$ ;  $\varepsilon = 0.73$  and  $L = 9.5 \text{ cm}$ .

In addition, the adsorption capacity of the Tururi fibers also increases with the increase in the adsorbent bed height.

Fig. 4 displays the numerical results of the multielement breakthrough curves of the metal ions using a concentration,  $C_{in}$ , of  $300 \text{ mg L}^{-1}$  for each metal ions, a bed height,  $L$ , of  $9.5 \text{ cm}$ , and bed porosity of  $0.73$  for two different values of volumetric flow ( $Q = 8$  and  $4 \text{ mL min}^{-1}$ ). As the flow increases, the breakthrough times decrease.

The increase in flow rates implies a reduction in the hydraulic retention time (HRT) of the compounds

inside the column. According to Cooney [17], the HRT is a typical parameter of design and operation for fixed bed systems. Long residence times can lead to a decrease in metal ions removal, whereas shorter times do not allow an effective contact between Tururi fibers and metal ions. The HRT is given by the ratio between the volume of the column and the flow.

As the flow increases, the breakthrough times of the metal ions compounds decrease as well the adsorption capacity of the Tururi fiber for each metal ions. The increase in flow rates implies a reduction in the HRT of the compounds inside the column.

Fig. 5 displays the numerical results of the multielement breakthrough curves of the metal ions using a concentration,  $C_{in}$ , of  $300 \text{ mg L}^{-1}$  for each metal ions, a bed height,  $L$ , of  $9.5 \text{ cm}$ , and a volumetric flow rate of  $4 \text{ mL min}^{-1}$  for two different values of the bed porosity ( $\varepsilon = 0.73$  and  $0.53$ ). According to Vidal et al. [8], as the porosity of the bed increases, the void space also increases, thus decreasing the number of active sites inside the column. As a result, the adsorption capacity of the bed is smaller than the breakthrough times. This effect was most pronounced for the compounds whose rupture time was increased.

In all cases, it can be observed that the sorbent has an affinity order that follows:  $\text{Cd}^{2+} > \text{Cu}^{2+} > \text{Ni}^{2+} = \text{Pb}^{2+}$ . For cadmium and cooper, due to high affinity for these metal ions, saturation was not completely reached and the bed still has free active sites that can adsorb them. On the other hand, for nickel and lead ions, the saturation is earlier reached and at this point starts to desorb. In the beginning of the adsorption process, the active

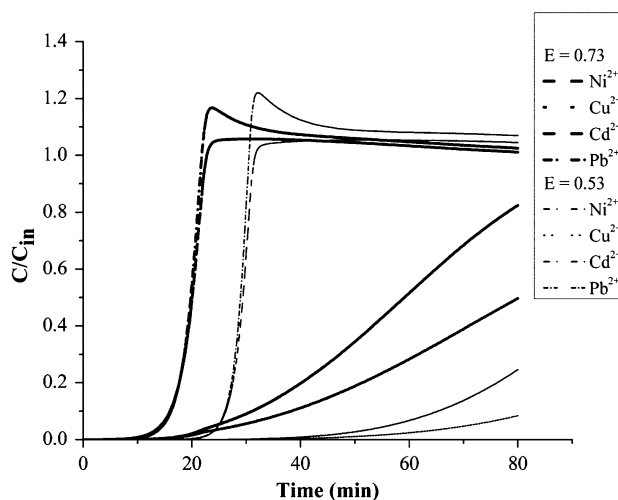


Fig. 5. Breakthrough curves of the metal ions for two different bed porosities. Initial conditions:  $C_{in} = 300 \text{ mg L}^{-1}$ ;  $Q = 4 \text{ mL min}^{-1}$  and  $L = 9.5 \text{ cm}$ .

Table 3  
Content of the elements based on XRF analysis

Element	Initial Tururi (%)	Tururi–Pb <sup>2+</sup> (%)	Tururi–Cu <sup>2+</sup> (%)	Tururi–Cd <sup>2+</sup> (%)	Tururi–Ni <sup>2+</sup> (%)
K	37.336	–	–	25.07	0.5181
Ca	31.745	0.7013	2.2335	14.147	3.592
Si	12.151	–	2.4967	–	3.473
Mn	5.1284	–	–	–	–
Al	4.3314	–	1.7516	–	2.3132
Cl	2.7653	–	–	–	0.1379
Fe	2.7542	0.2884	0.1793	–	0.3141
S	1.9895	–	–	–	0.5385
P	1.8001	–	–	–	–
Pb	–	98.777	–	4.8766	–
Cu	–	–	93.341	–	1.3909
Cd	–	–	–	55.906	–
Ni	–	0.2335	–	–	87.722

sites are available and in large amount. Over time, the competition effect takes place and metal ions that had low affinity starts to desorb at this point, increasing their concentrations in the fluid phase and overcoming the influent concentration. The ions that had high affinity occupy those active sites and the saturation is reached latter. Similar results were found by [8,16].

In order to formulate the hypothesis why the Tururi fibers are a good adsorbent for metal ions, the chemistry of the surface of the initial adsorbent and that after adsorption was analyzed. Table 3 shows X-ray fluorescence results, which were performed to identify and quantify the elements that were present in both adsorbents (before and after adsorption). As expected, sodium and calcium losses were observed in the exhausted samples compared to the initial one due to the exchange of those ions with the metal ions species. According to the results, an amount of 98.8, 93.3, 55.9, and 87.7% of Pb<sup>2+</sup>, Cu<sup>2+</sup>, Cd<sup>2+</sup>, and Ni<sup>2+</sup>, respectively, was incorporated to the Tururi fibers after adsorption process.

#### 4. Conclusions

An experimental and numerical study of adsorption of metal ions on Tururi fibers in aqueous solution was carried out. The multicomponent Langmuir model was used to describe the equilibrium in the multicomponent system. The kinetics in a batch reactor showed that the multicomponent adsorption equilibrium was reached instantaneous. The numerical results presented a good agreement in relation to experimental data for the multicomponent breakthrough curves. With an increase in the bed height,

the breakthrough times of the metal ions increased. As the flow increased, the breakthrough times of the metal ions underwent a decrease. The adsorption process was represented with good accuracy by the mathematical model and the numerical methodology used, allowing other situations to be simulated.

#### References

- [1] C. Baird, M. Cann, Environmental Chemistry, fifth ed., Freeman and Company, New York, NY, 2012.
- [2] D.Q. Melo, V.O.S. Neto, J.T. Oliveira, A.L. Barros, E.C.C. Gomes, Adsorption equilibria of Cu<sup>2+</sup>, Zn<sup>2+</sup>, and Cd<sup>2+</sup> on EDTA-functionalized silica spheres, *J. Chem. Eng. Data* 58 (2013) 798–806.
- [3] G.S.C. Raulino, C.B. Vidal, A.C.A. Lima, D.Q. Melo, J.T. Oliveira, R.F. Nascimento, Treatment influence on green coconut shells for removal of metal ions: Pilot-scale fixed-bed column, *Environ. Technol.* 35 (2014) 1711–1720.
- [4] M.A. Hubbe, S.H. Hasan, J.J. Ducoste, Cellulosic substrates for removal of pollutants from aqueous systems: A review, *Met. Bioresour.* 6 (2011) 2161–2287.
- [5] R.A. Sanchez, B.P. Espósito, Preparation of sugarcane bagasse modified with the thiophosphoryl function and its capacity for cadmium adsorption, *Bioresour* 6 (2011) 2448–2459.
- [6] S.A. Moreira, F.W. Sousa, A.G. Oliveira, R.F. Nascimento, E.S. de Brito, Metal removal from aqueous solution using cashew bagasse, *Quim. Nova* 32 (2009) 1717–1722.
- [7] V.O.S. Neto, T.V. Carvalho, S.B. Honorato, C.L. Gomes, F.C. Freitas, M.A.A. Silva, P.T.C. Freire, R.F. Nascimento, Coconut bagasse treated by thiourea/ammonia solution for cadmium removal: Kinetics and adsorption equilibrium, *Bioresour* 7 (2012) 1504–1524.
- [8] C.B. Vidal, G.S.C. Raulino, A.D. da Luz, C. da Luz, R.F. do Nascimento, D. de Keukeleire, Experimental

- and theoretical approach to multicomponent adsorption of selected aromatics on hydrophobically modified zeolite, *J. Chem. Eng. Data* 59 (2014) 282–288.
- [9] D.M. Ruthven, *Principles of Adsorption and Adsorption Processes*, Wiley, New York, NY, 1984.
- [10] D.Q. Melo, C.B. Vidal, A.L. Silva, R.N.P. Teixeira, G.S.C. Raulino, T.C. Medeiros, P.B.A. Fechine, S.E. Mazzeto, D. Keukeleire, R.F. Nascimento, Removal of  $\text{Cd}^{2+}$ ,  $\text{Cu}^{2+}$ ,  $\text{Ni}^{2+}$ , and  $\text{Pb}^{2+}$  ions from aqueous solutions using tururi fibers as an adsorbent, *J. Appl. Polym. Sci.* 131 (2014) 40883, doi: [10.1002/app.40883](https://doi.org/10.1002/app.40883).
- [11] D. Chatzopoulos, A. Varma, Aqueous-phase adsorption and desorption of toluene in activated carbon fixed beds: Experiments and model, *Chem. Eng. Sci.* 50 (1995) 127–141.
- [12] R.K. Gautam, A. Mudhoo, G. Lofrano, M.C. Chattopadhyaya, Biomass-derived biosorbents for metal ions sequestration: Adsorbent modification and activation methods and adsorbent regeneration, *J. Environ. Chem. Eng.* 2 (2014) 239–259.
- [13] D.D. Maksin, A.B. Nastasović, A.D. Milutinović-Nikolić, L.T. Suručić, Z.P. Sandić, R.V. Hercigonja, A.E. Onjia, Equilibrium and kinetics study on hexavalent chromium adsorption onto diethylene triamine grafted glycidyl methacrylate based copolymers, *J. Hazard. Mater.* 209–210 (2012) 99–110.
- [14] R.N.P. Teixeira, V.O. Sousa Neto, J.T. Oliveira, D.Q. Melo, M. A. Silva, R.F. Nascimento, Study on the use of roasted barley powder for adsorption of  $\text{Cu}^{2+}$  ions in batch experiments and in fixed-bed columns, *Biore-sources* 8 (2013) 3356–3573.
- [15] V.O. Sousa Neto, D.Q. Melo, T.C. de Oliveira, R.N.P. Teixeira, M.A.A. Silva, R.F. Nascimento, Evaluation of new chemically modified coconut shell adsorbents with tannic acid for Cu (II) removal from wastewater, *J. Appl. Polym. Sci.* 131 (2014) 40744, doi: [10.1002/app.40744](https://doi.org/10.1002/app.40744).
- [16] A.H. Sulaymon, K.W. Ahmed, Competitive adsorption of furfural and phenolic compounds onto activated carbon in fixed bed column, *Environ. Sci. Technol.* 42 (2008) 392–397.
- [17] D.O. Cooney, *Adsorption Design for Wastewater Treatment*, CRC Press, Boca Raton, FL, 1999.
- [18] A.D. Luz, S.M. Guelli Ulson de Souza, C. da Luz, R.V. de Paula Rezende, A.A. Ulson de Souza, A.A.U. Souza, Multicomponent adsorption and desorption of BTX compounds using coconut shell activated carbon: Experiments, mathematical modeling, and numerical simulation, *Ind. Eng. Chem. Res.* 52 (2013) 7896–7911.